Project Report for fulfillment of

PH4103: Condensed Matter Laboratory

By

Vishal Singh

16MS007

Under the supervision of

Dr. Bhavtosh Bansal

Indian Institute of Science Education and Research, Kolkata

Mohanpur, West Bengal 741246

Contents

List of Figures

1 Experiment 1- Experimental verification of the Kramers–Kronig relations

1.1 Lock-In Amplifier

1.1.1 Theory

The phase sensitive or "lock-in" amplifier is a common instrument used in solving signal-to-noise problems in research laboratories. It is a very powerful instrument where signals of interest can be detected even if they are smaller than the noise signals they accompany. Lock-in amplifiers are also used to detect and measure very small AC signals—down to nanovolts or smaller where noise is always a concern. Lock-in amplifiers use a technique known as phase sensitive detection to single out the component of the signal at a specific frequency and phase. Once it does this, noise signals at other frequencies or random phases are rejected through electronic (analog lockin) or software (DSP lock-in) filtering.

1.1.2 Working

The lock-in amplifier is used to detect a modulated signal (i.e., a signal that oscillates at a well defined frequency and phase) that is typically buried in a large noise background. To do so, a reference signal (i.e. a clean sinusoidal voltage whose frequency is the same as the one that you wish to detect) is supplied into the "lock-in." This reference provides both the frequency and phase of the expected signal. To narrow its output to a small bandwidth around the expected frequency at the specified phase, the signals are multiplied together (a.k.a. mixed or demodulated). If the signal and reference are correlated their multiplication will be positive on average since a positive number times a positive number and a negative number times a negative number are both result in positive answers. Random noise and the reference are uncorrelated and their multiplied value will fluctuate in time and average to zero. A low pass filter picks out the part of the signal that is correlated with the reference essentially by averaging the output of the mixer, This is the lock-in output. A setting on the low pass filter (the time constant) sets how long this averaging is done (and the inverse of the time constant is the bandwidth of the measurement).

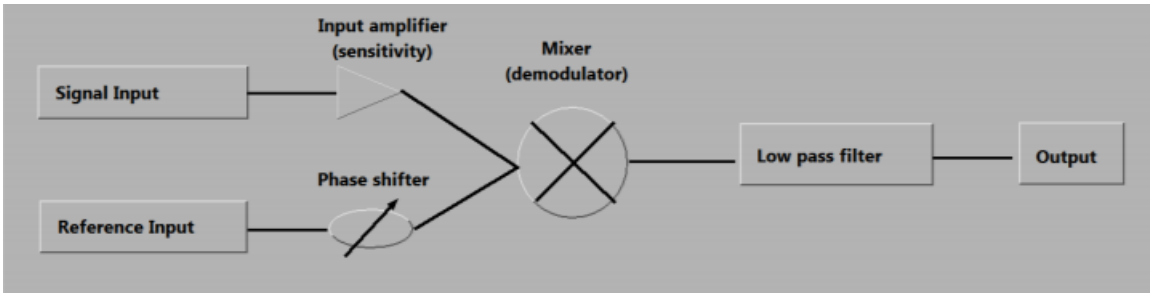

Figure 1: Block Diagram of a Lock-in Amplifier.

1.1.3 Mathematics

Lock-in measurements require the input signal to oscillate at the reference frequency. Thus, typically an experiment is excited (or modulated) at a fixed frequency (from an oscillator or function generator) and the lock-in amplifier detects the response from the experiment. Suppose the reference signal is a square wave at frequency ωR. This might be the sync output from a function generator. If the sine output from the function generator is used to excite the experiment, the response might be $V_I sin(\omega_R t + \theta_I)$ where V_I is the signal amplitude.

Using the square wave, the lock-in then creates an internal reference $V_R sin(\omega_R t + \theta_R)$ and multiplies the signal by the reference using a mixer. The mixer generates the product of its two inputs as its output V_{MI}.

$$V_{MI} = V_I V_R sin(\omega_R t + \theta_I) sin(\omega_R t + \theta_R) \tag{1}$$

or

$$V_{MI} = \frac{1}{2} V_I V_R cos(\theta_R - \theta_I) + \frac{1}{2} V_I V_R sin(2\omega_R t + \theta_R + \theta_I) \tag{2}$$

Since the two inputs to the mixer are at exactly the same frequency, the first term in the mixer output is at DC (time independent) or $cos(\theta_R - \theta_I)$. The second term is at frequency $2\omega_R$ which is a high frequency and can be readily removed using a low pass filter. After filtering,

$$V_{MI+FILT} = \frac{1}{2} V_I V_R cos(\theta_R - \theta_I) \tag{3}$$

which is proportional to the cosine of the phase difference between the input and the reference. Hence the term phase-sensitive detection.

In order to measure V_I using equation (3), the phase difference between the signal and reference, $\theta_R - \theta_I$, must be stable and known. The lock-in amplifier solves this problem by using two mixers, with the reference inputs 90^0 out of phase. The reference input to the second mixer is $V_R sin(\omega_R t + \theta_R - \pi/2)$ and the output of the second mixer is:

$$V_{M2} = \frac{1}{2} V_I V_R cos(\theta_R - \theta_I - \pi/2) + \frac{1}{2} V_I V_R sin(2\omega_R t + \theta_R + \theta_I - \pi/2) \quad (4)$$

After filtering,

$$V_{M2+FILT} = \frac{1}{2} V_I V_R cos(\theta_R - \theta_I - \pi/2) = \frac{1}{2} V_I V_R sin(\theta_R - \theta_I) \quad (5)$$

The amplitude and phase (compared to the reference) of the input signal can be determined from the two mixer outputs, equations (3) and (5). The result is:

$$Amplitude : R = (2/V_R)\sqrt{V_{MI+FLT}^2 + V_{M2+FLT}^2} \quad (6)$$

$$Phase : \theta_R - \theta_I = tan^{-1}\left(\frac{V_{M2+FLT}}{V_{MI+FLT}}\right) \quad (7)$$

1.2 The Kramers-Kronig Relations

The Kramers-Kronig Relations gives us the relation between the real and the imaginary parts of dielectric functions, relations that are actually independent of the assumption of thermal equilibrium, unlike fluctuation-dissipation theorem. The theorem considers the much weaker assumption of causality (A causal function is one whereby the response to an excitation depends only on the past, not on the future.)

Dispersion relations are relations between physical quantities which hold, in general, for every linear, time-independent, causal physical system. Therefore, we shall formulate them in a somewhat more abstract manner for a cause U(t) and an effect E(t), and later on, explain them for some examples of interest to us. The quantities U(t) and E(t) are assumed to be real physical quantities which are connected by some physical process, not necessarily an electromagnetic one. But this process of connection has to he linear, time-independent, and causal. Examples for such U(t) and E(t) are the electric field E(t) or the polarization P(t), respectively, at a certain point in a piece

of matter. Another example is the current I in a circuit caused by a generator of voltage V, which is the case that we have considered in our calculation.

For an LCR circuit in series, we have:

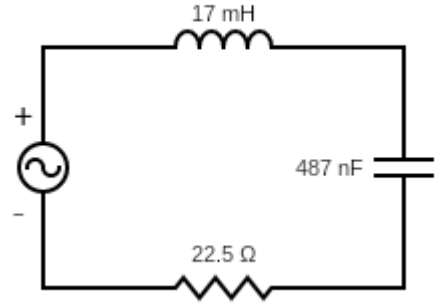

Figure 2: Schematic of circuit used for experiment.

$$L\frac{dI}{dt} + \frac{Q}{C} + RI = V$$
$$L\frac{d^2Q}{dt^2} + \frac{Q}{C} + R\frac{dQ}{dt} = 0$$

Here, $I = dQ/dt$. This is analogous relation to a damped oscillator. The solution: $Q(t) = Q(\omega)e^{-iwt}$

Since $I = dQ/dt$, $I(\omega) = -i\omega Q(\omega)$

$$g(\omega) = \frac{I(\omega)}{V(\omega)} = \frac{1}{Z} \tag{8}$$

where $Z = -i\omega L + R + \frac{i}{\omega C}$. In this case the transfer function $g(\omega)$ is $Y(\omega) = 1/Z$. It is also called the admittance of the circuit.

Now, we take the general consideration of $U(t)$ and $E(t)$ in Fourier form:

$$U(t) = \frac{1}{\sqrt{2\pi}}\int_{-\infty}^{\infty} d\omega e^{-i\omega t}u(\omega) \tag{9}$$
$$E(t) = \frac{1}{\sqrt{2\pi}}\int_{-\infty}^{\infty} d\omega e^{-i\omega t}e(\omega) \tag{10}$$

Next, we use the assumption that the relation between the cause $U(t)$ and the effect $E(t)$ is linear. This implies the following: If the cause U_1 gives rise to the effect E_1, and U_2 gives rise to the effect E_2 then $\alpha U_1 + \beta U_2$ causes the effect $\alpha E_1 + \beta E_2$. This property of linearity may be summarized in the following form:

$$E(t) = \int_{-\infty}^{\infty} dt' G(t, t') U(t') \tag{11}$$

where $G(t, t')$ is a weight function that weights the distinct causes at time t' contributing to the effect at time t. Hence, studying the physical system with respect to cause and effect is equivalent to the investigation of the Green function $G(t, t')$.

The next property of the physical process to be taken into account is that this physical process, connecting cause and effect, should itself be independent of the time at which it proceeds. This implies that $G(t, t')$ can be a function of the time-difference $t - t'$ only; then,

$$E(t) = \int_{-\infty}^{\infty} dt' G(t - t') U(t') \tag{12}$$

From Fourier Transform,

$$G(t) = \frac{1}{2\pi} \int_{-\infty}^{\infty} d\omega e^{-i\omega t} g(\omega) \tag{13}$$

Using this result in our case,

$$g(\omega) = \int_{-\infty}^{\infty} dt e^{i\omega t} G(t) = \int_{0}^{\infty} dt e^{i\omega t} G(t) \tag{14}$$

The same equation may be used to extend the definition of $g(\omega)$ to complex frequencies $\omega = \omega_1 + i\omega_2$ Then one can also expect that $g(\omega)$ possesses no singularities in the upper complex ω-half-plane if $g(\omega)$ behaves reasonably along the real ω-axis. To better understand the sense of the extension of the definition of $g(\omega)$ to complex ω-values in the upper half-plane we compare:

$$g(\omega_1) = \int_{0}^{\infty} dt e^{i\omega_1 t} G(t) \tag{15}$$

$$g(\omega_1 + i\omega_2) = \int_{0}^{\infty} dt e^{i\omega_1 t} G(t) e^{-i\omega_2 t} \tag{16}$$

For complex ω the integrand is smaller bt the factor $e^{-\omega_2 t}$. if ω lies in the upper half-plane, then $\omega_2 > 0$ and therefore always $0 \leq e^{-\omega_2 t} \leq 1$. For the derivation, we get:

$$\left(\frac{dg}{d\omega}\right)_{\omega=\omega_1+\omega_2} = \int_0^\infty dt e^{i\omega_1 t} G(t) i t e^{-\omega_2 t} \tag{17}$$

In general, this derivative exists in the upper half-plane, supposing $g(\omega)$ is finite on the real axis: although the integrand, compared to (15), is multiplied by it the factor $e^{-\omega_2 t}$ will suppress any power of t for long times. Now, if the derivative of a complex function exists in the neighborhood of a point in the complex plane, then the function is analytic at this point. Due to these considerations we may conclude that the derivative of $g(\omega)$ exists everywhere in the upper half-plane, and therefore, the function $g(\omega)$ is analytic in the entire upper half-plane. This implies that for a linear, time-independent, and causal system the Fourier transform of the Green function $G(t)$ (transfer function) $g(\omega)$ originally defined for real ω equals the limiting value of a function g of complex argument ω which is analytic in the entire upper half-plane.

The dispersion relations are derived from the line integral:

$$\int d\omega' \frac{g(\omega')}{\omega' - \omega} \tag{18}$$

taken along the real axis (possibly shifted into the upper half-plane) and a semicircle of radius R lying in the upper half-plane.

$g(\omega)$ has no singularities in the interior and on the boundary of this closed curve. Therefore, with ω on the real axis, $g(\omega')/(\omega' - \omega)$ is also analytic in the domain mentioned; hence, the integral (18) vanishes. Now, it is further assumed that $g(\omega)$ behaves such (that is, that the physical system considered behaves in such a manner) that the part of the integral (18) along the upper semicircle vanishes as $R \longrightarrow \infty$, but this is not always the case.

This quantity has a pole on the real line $\omega = \omega'$ (along with other poles in the lower half-plane). Now, as $R \to \infty$, the semicircle C of the order $\frac{2\pi R}{R^3} \to 0$, or

$$0 = \int_C d\omega' \frac{g(\omega')}{\omega' - \omega} = \int_{-\infty}^{\infty} d\omega' \frac{g(\omega')}{\omega' - \omega} + \int_{arc} d\omega' \frac{g(\omega')}{\omega' - \omega} \tag{19}$$

$$= \int_{-\infty}^{\infty} d\omega' \frac{g(\omega')}{\omega' - \omega} = P \int_{-\infty}^{\infty} d\omega' \frac{g(\omega')}{\omega' - \omega} - i\pi g(\omega) \tag{20}$$

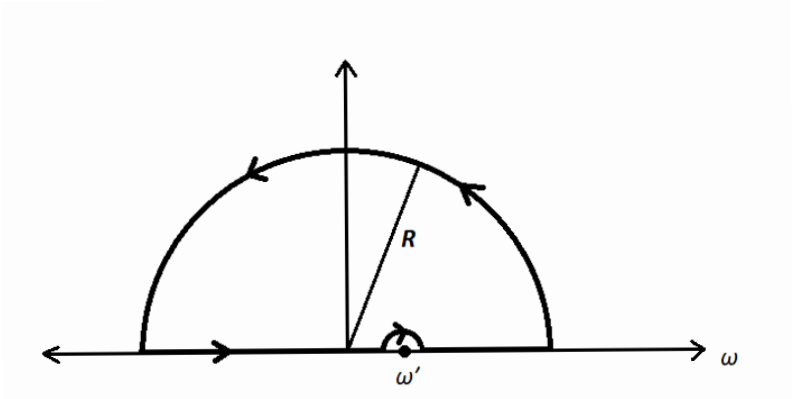

Figure 3: Illustration of the integration path used in eq (17)

From this, we get:

$$g(\omega) = \frac{1}{i\pi} P \int_{-\infty}^{\infty} d\omega' \frac{g(\omega')}{\omega' - \omega} \tag{21}$$

If we look at the expression, we see that, both the LHS and inside the integration, we get the $g(\omega)$ term. But the integration term is preceded by an i, which is the root of the relation between the real and imaginary part of $g(\omega)$.

We get,

$$Re[g(\omega)] = \frac{1}{\pi} P \int_{-\infty}^{\infty} d\omega' \frac{Im[g(\omega')]}{\omega' - \omega} \tag{22}$$

$$Im[g(\omega)] = -\frac{1}{\pi} P \int_{-\infty}^{\infty} d\omega' \frac{Re[g(\omega')]}{\omega' - \omega} \tag{23}$$

These equations are called the **Dispersion Relations**. The characteristic of this equation is to connect the real and imaginary part of $g(\omega)$.

Now, we induce the condition of symmetry, i.e. $g(\omega) = g^*(-\omega)$.

$$
\begin{aligned}
Re[g(\omega)] &= \frac{1}{\pi} P \int_{-\infty}^{\infty} d\omega' \frac{Im[g(\omega')]}{\omega' - \omega} \\
&= Re[g(-\omega)] \\
&= \frac{1}{\pi} P \int_{-\infty}^{\infty} d\omega' \frac{Im[g(\omega')]}{\omega' + \omega} \\
Im[g(\omega)] &= -\frac{1}{\pi} P \int_{-\infty}^{\infty} d\omega' \frac{Re[g(\omega')]}{\omega' - \omega} \\
&= -Im[g(-\omega)] \\
&= -\frac{1}{\pi} P \int_{-\infty}^{\infty} d\omega' \frac{Re[g(\omega')]}{\omega' + \omega}
\end{aligned}
$$

Therefore,

$$
Im[g(\omega)] = -\frac{2\omega}{\pi} P \int_{0}^{\infty} d\omega' \frac{Re[g(\omega')]}{\omega'^2 - \omega^2} \tag{24}
$$

$$
Re[g(\omega)] = \frac{2}{\pi} P \int_{0}^{\infty} d\omega' \frac{\omega' Im[g(\omega')]}{\omega'^2 - \omega^2} \tag{25}
$$

These two equations are called the **Kramers-Kronig dispersion relations**.

1.3 Results

The aim of our experiment was to experimentally verify to Kramers Kronig relations. To achieve this, we chose to work in the environment of an LCR circuit (fig 2). The quantity used for this verification of the relations was the Admittance of the circuit. It has both real and imaginary components. So we experimentally tabulated both the real and imaginary values of admittance of the circuit using a Lock-In Amplifier. Then, we used the amplitude of real component of the admittance along with the Kramers Kronig relations to "calculate" the amplitude of the imaginary component of the admimttance. We then proceeded to plot both the experimentally calculated amplitude and the amplitude calculated through the Kramers Kronig relations. Similar treatment was also done to the experimentally gotten amplitude of the imaginary component of admittance to calculate the amplitude of the real component of admittance.

We observed a very good agreement of experimentally obtained data and data calculated using Kramers Kronig relation for amplitudes of both real

and imaginary components of admittance of the circuit. Even on the log-log scale, it is difficult to differentiate the calculated and observed amplitudes. The plots are shown below.

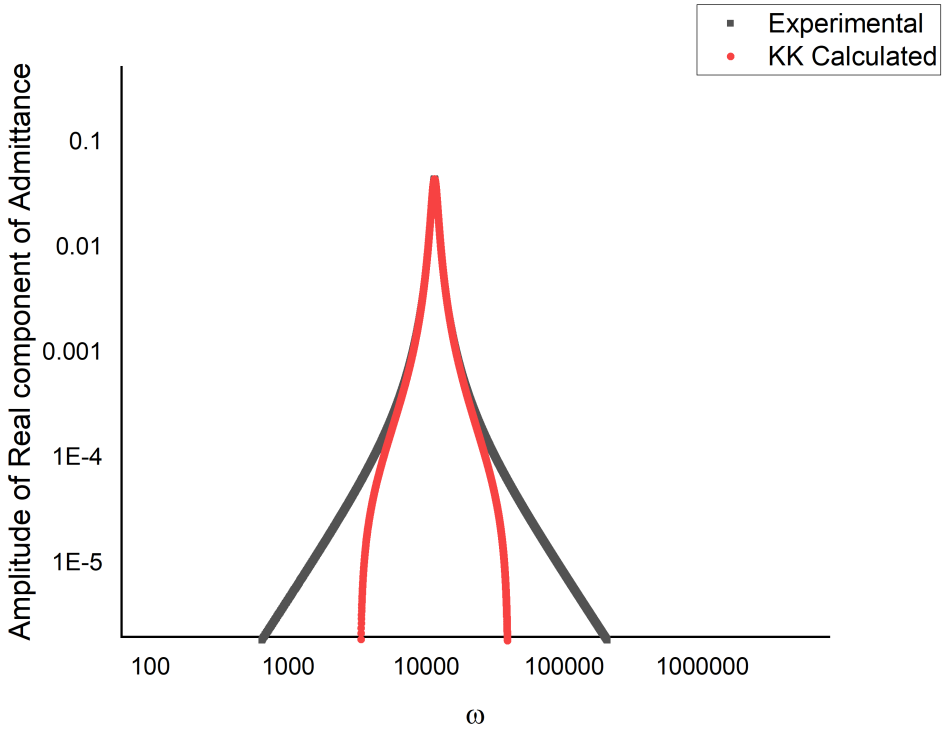

Figure 4: Comparison of Amplitude of real component of admittance (experimental results and data calculated using Kramers Kronig Relations).

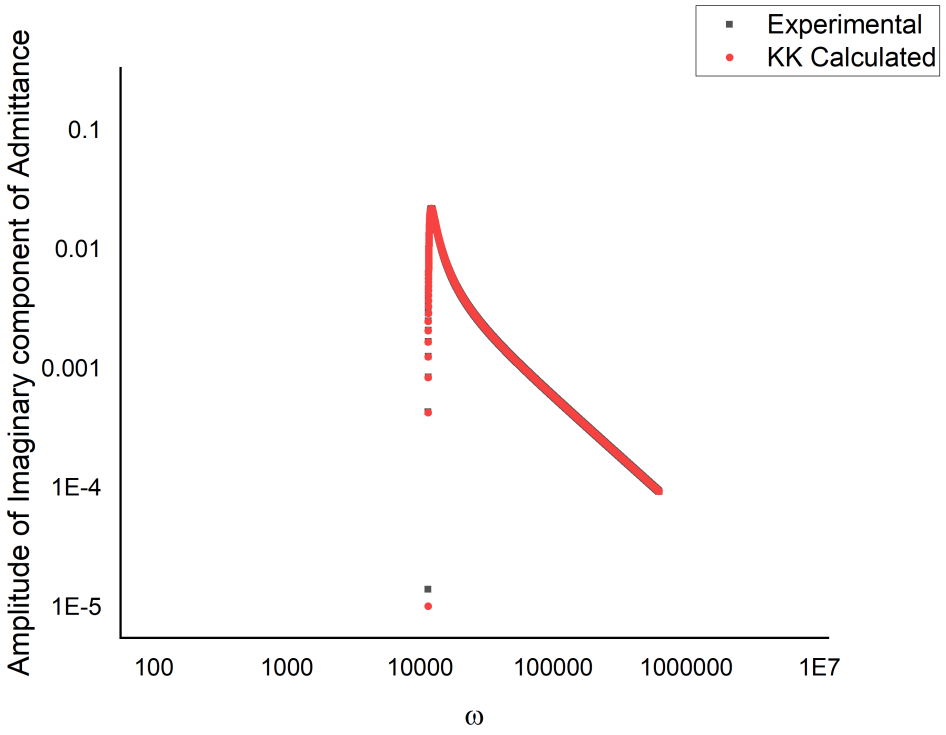

Figure 5: Comparison of Amplitude of imaginary component of admittance (experimental results and data calculated using Kramers Kronig Relations).

1.4 Discusssion

The LCR circuit we have used in our experiment is analogous to many optical materials, when it comes to systems with balanced loss and gain regions. The concept of these systems stems from the idea of the extension of quantum mechanics to non-Hermitian Hamiltonians possessing PT-symmetry. PT-symmetrical systems are invariant with respect to the simultaneous spatial inversion and time inversion. The former performed by the linear operator $\hat{P}$ which transforms coordinates and momenta as $r \longrightarrow -r$ and $p \longrightarrow -p$, while the time inversion is performed by the antilinear operator $\hat{T}$, which transforms $p \longrightarrow -p$ and $i \longrightarrow -i$; the simultaneous application of these operators, $\hat{P}\hat{T}$ antilinear, it transforms $r \longrightarrow -r$, $p \longrightarrow -p$ and $i \longrightarrow -i$.

In optics, PT-symmetry is usually studied in the frequency domain by

considering solutions of the scalar Helmholtz equation for the z-component of the electric field E:

$$\left(\frac{\partial^2}{\partial x^2}+\frac{\partial^2}{\partial y^2}+\frac{\omega^2}{c^2}\varepsilon(\omega,x,y)\right)E(\omega,x,y)=0 \tag{26}$$

A system is PT-symmetrical if and only if (26) is invariant with respect to the $\hat{P}\hat{T}$- transformation. This happens if $\varepsilon(\omega,x)$ satisfies (26).

$$Re(\varepsilon(\omega,x))=Re(\varepsilon(\omega,-x)) \tag{27}$$

$$Im(\varepsilon(\omega,x))=-Im(\varepsilon(\omega,-x)) \tag{28}$$

In any optical system with either loss or gain, frequency dispersion of the permittivity is crucial. Due to causality, a dielectric function $\varepsilon(\omega,x)$ must be analytic in the upper half of the complex frequency plane so that all its singularities are situated in the lower half of the complex plane, just as the calculations we did in the Kramers-Kronig relation derivation. Causality must hold for both dissipative and active systems. Due to this causality principle, $\varepsilon(\omega,x)$ must satisfy the Kramers-Kronig relations.

As an example, let us consider a medium described by dielectric permittivity as given below:

$$\varepsilon(\omega)=\varepsilon_{\mathrm{m}}-\frac{\alpha}{\omega^2-\omega_0^2+2i\gamma\omega} \tag{29}$$

Here, $\varepsilon_{\mathrm{m}}$is a dielectric permittivity of the matrix in which amplifying (absorbing) media are placed, α and γ are the strength and the linewidth of amplification (absorption), respectively. For an absorbing medium $Im(\varepsilon)>0$, thus α and γ must be positive. For an amplifying medium, $Im(\varepsilon)<0$, so that one of the parameters α or γ must be negative. For real frequencies, negative γ is equivalent to the complex conjugation of $\varepsilon(\omega)$. This corresponds to moving the pole of $\varepsilon(\omega)$ from the lower to the upper half of the complex frequency plane. The latter violates causality for the response function. Therefore, the only choice for parameters α and γ is $\alpha<0$ and $\gamma>0$, which corresponds to the "antiresonance" of the real part of the dielectric function [20]. The choice $\alpha<0$ and $\gamma>0$ ensures causality but is incompatible with PT-symmetry. Indeed, as shown in Fig. 6, when condition (26) is satisfied, due to resonant behavior of the absorbing medium and antiresonant behavior of the amplifying medium, condition (27) can hold at one point, $\omega=\omega'$, only. This illustrates the general rule following from the Kramers-Kronig relations.

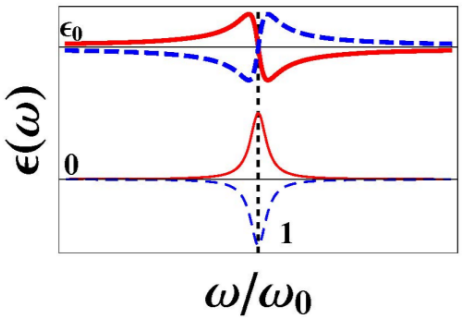

Figure 6: Real (thick lines) and imaginary (thin lines) parts of dielectric permittivity of absorbing (solid lines) and amplifying (dashed lines) media dielectric permittivities are given by Eq. (29) with opposite signs of the imaginary parts.

We can witness a similar trend in our case of admittance. The graph:

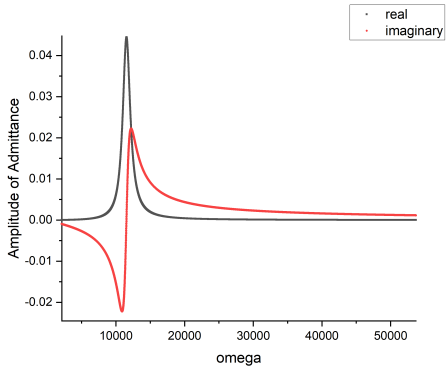

Figure 7: The graphs of real and imaginary parts of admittance that we got from experiment

The graph that we got, is for the case when the LCR is functioning as a loss medium. The graphs invert, just as in Fig. (6), when we solve the LCR for a medium with gain. Thus, LCR is analogous to the optical medium, as the trend of loss and gain in LCR is reflected in the absorbance and amplification of the optical medium. In fact, if we see the derivation of the Kramers-Kronig relation, we see that this is the case for any medium where we see an equation resembling the damped harmonic oscillator. And this trend can be shown using PT-symmetry. This is a very powerful result.

Code for interfacing with the Lock-in amplifier and taking data (here, we have typed the code for 900Hz to 5KHz range. In fact, this is a general code that can be edited to function in any range, given the sensitivity):

```
    clc; clear;

L=gpib('keithley',0,12); %Lock-in address=12
fopen(L);

fa=zeros(4100,1);
theta=zeros(4100,1);
fprintf(L, 'SENS 17');
pause(2);    %After changing sensitivity, it is better to wait for 2 sec,
             %to avoid incorrect reading
q=1;
for i = 901:5000
    fprintf(L, 'FREQ %d',i);
    theta(q)=i;
    if i== 1787
        fprintf(L, 'SENS 18');
        pause(2);
    end
    if i==1885
        fprintf(L, 'SENS 17');
        pause(2);
    end
    fa(q)=(str2double(query(L,'OUTP?3')));
    q=q+1;
end


fclose(L);
delete(L);
plot(theta, fa);
```

This page is intentionally left blank.

2 Experiment 2- Linking Thermodynamics and Information by the experimental verification of Landauer's Principle

2.1 Introduction

In 1961, Rolf Landauer argued that erasure of information is a dissipative process. It says "Any logically irreversible manipulation of information, such as the erasure of a bit or the merging of two computation paths, must be accompanied by a corresponding entropy increase in non-information-bearing degrees of freedom of the information-processing apparatus or its environment." In this experiment, we aim to experimentally realize the existence of Landauer's bound in the generic model of a one-bit memory. The way to go about this is to trap a single colloidal particle in a double-well potential, which is similar to the original work of Landauer.

2.2 Maxwell's Demon

Maxwell's demon is a thought experiment that illustrates the probabilistic nature of the second law of thermodynamics. James Clerk Maxwell introduced it to the public in 1871 in his book Theory of Heat. The demon is an intelligent agent or creature capable of measuring the speed of individual molecules in a gas. The gas is split into two vessels connected by a door, where both vessels are at the same pressure and temperature, and the entire system is in equilibrium. The demon can also open and close the door and allow fast molecules to pass to the right chamber and slow molecules to the left. It keeps repeating this process until the majority of the slow molecules are on the left and fast ones are on the right. This creates a temperature gradient, and one could potentially use that gradient for extracting work. Essentially, the demon took the isolated system out of thermal equilibrium, without doing work, which contradicts the second law of thermodynamics. Maxwell's demon is the first discussion of the role that feedback plays in thermodynamics, showing how the demon's measurement based on the acquired information can alter the thermodynamics of a system.

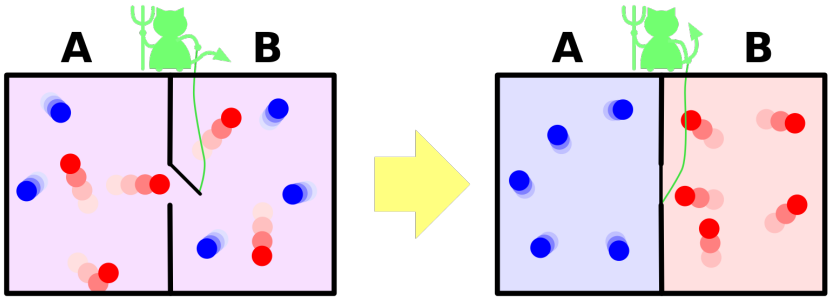

Figure 8: Schematic figure of Maxwell's demon thought experiment.

In fig 8 (a), the system is initially in thermal equilibrium. The demon can measure the speed of individual molecules and sort the fast and slow by opening the door between two vessels.In fig 8(b), sorting molecules creates a temperature difference in the system. The demon is therefore able to decrease the entropy of the system without performing any work himself, in apparent violation of the second law of thermodynamics.

The paradox of the apparent violation of the second law can be resolved by noting that during a full thermodynamic cycle, the memory of the demon, which is used to record the coordinates of each molecule, has to be reset to its initial state. Indeed, according to Landauer's principle, any logically irreversible transformation of classical information is necessarily accompanied by the dissipation of at least $k_\beta Tln(2)$ of heat per lost bit where k is the Boltzmann constant and T is the temperature.

2.3 The Idea

A device is said to be logically irreversible if its input cannot be uniquely determined from its output. Any Boolean function that maps several input states onto the same output state, such as AND, NAND, OR and XOR, is therefore logically irreversible. In particular, the erasure of information, the RESET TO ONE/NULL operation, is logically irreversible and leads to an entropy increase of $k_\beta ln2$ per erased bit. This entropy cost required to reset the demon's memory to a blank state is always larger than the initial entropy reduction, thus safeguarding the second law.

For the experimental verification, we plan to take the over-damped colloidal particle in a double-well potential. Our plan so far to go about this is to take charged beads and isolate a bead and trap it in a double-well potential by applying an electric field. Another way to go is to take silicon beads, and trap it using vertical optical tweezers. In both of these methods, we need to suspend the beads in a liquid medium, and take data of the Brownian motion observed.

Since presently we did not have beads to observe the Brownian motion and take readings, we resolved to the crude method to realize it, and used talcum particles instead, although the particles are much bigger in diameter (about $30\mu m$) than the beads we intended to use (about $2\mu m$). This shall atleast tell us about the accuracy of the calculation done for the estimation of the amplitude of the Brownian motion, and also the nature of the liquid suitable to execute the experiment.

2.4 Brownian Motion

Brownian motion or pedesis, is the random motion of particles suspended in a fluid resulting from their collision with the fast-moving molecules in the fluid.

This pattern of motion typically alternates random fluctuations in a particle's position inside a fluid sub-domain with a relocation to another sub-domain. Each relocation is followed by more fluctuations within the new closed volume. This pattern describes a fluid at thermal equilibrium, defined by a given temperature. Within such a fluid, there exists no preferential direction of flow as in transport phenomena. More specifically, the fluid's overall linear and angular momenta remain null over time. The kinetic energies of the molecular Brownian motions, together with those of molecular rotations and vibrations, sum up to the caloric component of a fluid's internal energy.

The many-body interactions that yield the Brownian pattern cannot be solved by a model accounting for every involved molecule. In consequence, only probabilistic models applied to molecular populations can be employed to describe it.

2.4.1 Brownian motion in macroscopic particles:

The more direct effects due to Brownian motion, such as thermal motion of free electron in the circuit cannot actually be observed experimentally; it is not possible to follow the motion of one individual electron or ion. But, light particles such as pollen grains, dust, or in our case beads and talcum will, however, exhibit a somewhat similar motion which can be visualised. As a matter of fact, this motion was first observed on a macroscopic level (powdered charcoal on alcohol) by a Dutch physician Jan Ingenhausz in 1785, but this phenomenon was named after a biologist, Robert Brown who, in 1827, gave an extensive report of his detailed investigations of the motion of pollen grains in water. Later, it was found out that it was due to the collisions with molecules of the surrounding fluid that were in thermal motion. Our current understanding tells us, that diffusion in thermal equilibrium is a random motion, mediated through collisions, i.e. it is a microscopic process. Mobility is a macroscopic quantity, but the origin of it has the same link: collisional interactions. In fact, **these microscopic fluctuating motion is not caused by thermal motion; it is thermal motion**

2.4.2 Calculation and estimation of the RMS of the amplitude of motion of the talcum particles

Langevin, soon after Einstein's work, presented in 1908 a different approach towards solving this problem, which was simpler. We shall proceed with his analysis.

Average diameter of a talcum particle, $a = 50\mu m$
Viscosity of water, $\eta = 8.9 \times 10^{-4} Pa$

There is a limitation to this analysis though; it only works for particles heavier than the liquid. We checked, and found out that the density of talcum is about 2.7 times the density of water, so we can use this analysis for calculation.

Assumption: the force on a particle is assumed to be composed of an average and fluctuating part $F(t)$, with $\langle F(t) \rangle = 0$. This gives:

$$M\frac{d^2x}{dt^2} = -6\pi\eta a\frac{dx}{dt} + F(t) \tag{30}$$

Here Langevin assumed that the coefficient to the average value $-\frac{d\langle x\rangle}{t}$ could be identified with the viscous drag given by the same formula as that in hydrodynamics, i.e. $-6\pi\eta a\nu$ where η is the dynamic viscosity of the liquid surrounding the particle, and a is the diameter of the particle, which is assumed to be spherical.

Multiplying by x on both sides, we get:

$$\frac{1}{2}M\frac{d^2(x^2)}{dt^2} - M(\frac{dx}{dt})^2 = -3\pi\eta a\frac{d(x^2)}{dt} + xF(t) \tag{31}$$

Since M is high (compared to the light particles such as the particles of the liquid medium), the particle does change its velocity, but very little after each collision. For the time interval of relevance ($> 10^{-8}$), we can assume that $F(t)$ is independent of x, i.e. $\langle xF(t)\rangle \simeq 0$.

Another assumption that we take here, is that, if x is known at time $t = 0$, then we can take $\langle x\rangle = 0$ and $\langle x^2\rangle = 0$. But, at $t = 0$, we do not have any information about dx/dt.

Since the particle is in thermal equilibrium with the surrounding medium, we have:

$$\langle(\frac{dx}{dt})^2\rangle = \langle u_x^2\rangle = \frac{k_\beta T}{M} \tag{32}$$

Here, we have considered for 2-dimensional case (since the colloidal particle is confined between a slide and a cover slip, the dimension along the z-direction is much higher than the x,y-direction, so it can be considered as a 2-dimensional case). We'll get the same expression for $\langle u_y^2\rangle$, assuming the medium is isotropic. Writing $\langle r^2\rangle = \langle u_x^2\rangle + \langle u_y^2\rangle$ we get:

$$\frac{1}{2}M\frac{d^2(\langle r^2\rangle)}{dt^2} + 3\pi\eta a\frac{d(\langle r^2\rangle)}{dt} = 2k_\beta T \tag{33}$$

$$\Rightarrow \quad \frac{d(\langle r^2\rangle)}{dt} = \frac{2k_\beta T}{3\pi\eta a} + Ce^{-6\pi\eta at/M} \tag{34}$$

Here, C is a constant determined by the initial conditions. For large times ($t >> M/6\pi\eta a$), we can ignore the exponential term, since it'll be really small.

We get,

$$\langle r^2\rangle = 2Dt \tag{35}$$

where,

$$D = \frac{k_\beta T}{3\pi\eta a} \tag{36}$$

From (31), we get:

$$\sqrt{\langle r^2 \rangle} = r_{RMS} = \sqrt{2Dt} \tag{37}$$

This equation gives us the RMS of the amplitude of the brownian motion.

After putting the values of D (calculated using the value of a and η given above) and $t \simeq 10sec$ in room temperature, we get,

$$r_{RMS} = 0.44 \times 10^{-6} m = 0.44 \mu m \tag{38}$$

One thing we should keep in mind that the particle that we used for this observation is too large. Ideally, it should have been $1/10^{th}$ the size of the particle we used, for us to track and quantify the data, with our calculated results. But this gives us an idea that the v_{RMS} shall exist in the μm to mm range, depending on the value of t.

2.5 Experimental Details

We tried to observe Brownian motion in talcum powder particles. We had access to a microscope with 100x magnification and 6x eyepiece lens, giving us a combined magnification of 600x. A visual study of the talcum powder particles kept on a layer of water (mixed with detergent to reduce surface tension, thereby reducing clumping) on a cover slip, showed us that the order of magnitude of the motion of particles was of the order of magnitude of the size of the particles(μm) which is in agreement of our calculation. We'd like to emphasize on the fact that this observation is done solely to verify the motion of the particles, and to establish a ground for the observation of brownian motion with charged beads.

2.6 What's Next?

As mentioned in the idea, we now aim to do this experiment with charged beads, isolate individual beads (by tracking their movement in the medium, which shall also tell us whether water is a good medium for the experiment or not) and trap them in a double-well potential applying an electric field. This way we will control the motion of the beads in z-direction and be able to better quantify their motion in the x-y plane. We'll have to consider the Brownian motion in the z-direction in our calculation too. Also, here we have used water as a medium.

Acknowledgement

We would like to thank our supervisor, Dr. Bhavtosh Bansal, who was extremely friendly and encouraging. This project was a great introduction to experimental condensed matter.

We are also thankful to Umesh Chandra Sahu whose LCR circuit was used for the experiments. A special thanks is also due for Tapas Bar and Kingshuk Mukhuti, who helped us in numerous ways throughout our work. Also, thanks to the second year bio lab for providing us with much needed equipment to carry out our experiments.

References

[1] Walter Greiner. *Thermodynamics and Statistical Mechanics.*

[2] Hans L. Pécseli. *Fluctuations in Physical Systems*

[3] Momčilo Gavrilov. *Experiments on the Thermodynamics of Information Processing*

[4] Antoine Bérut et al. *Experimental verification of Landauer's principle linking information and thermodynamics*

[5] A. A. Zyablovsky et al. *Causality and phase transitions in PT - symmetrical optical systems*